Available online at www.sciencedirect.com
SCIENCE DIRECT®
Journal of Molecular Catalysis A: Chemical 214 (2004) 273–279
JOURNAL OF MOLECULAR CATALYSIS A: CHEMICAL
www.elsevier.com/locate/molcata

Characterization and catalytic activity of TiO_2/SiO_2 for transesterification of dimethyl oxalate with phenol

Shengping Wang, Xinbin Ma*, Hongli Guo, Jinlong Gong, Xia Yang, Genhui Xu

State Key Laboratory of C_1 Chemistry and Technology, School of Chemical Engineering and Technology, Tianjin University, Weijin Road 92, Nankai District, Tianjin 300072, China

Received 15 July 2003; received in revised form 19 December 2003; accepted 21 December 2003

Abstract

The transesterification of dimethyl oxalate (DMO) with phenol to produce methyl phenyl oxalate (MPO) and diphenyl oxalate (DPO) was carried out over TiO_2/SiO_2 catalyst. The evaluation results showed that TiO_2/SiO_2 had better activity and excellent selectivity to target products compared with many conventional ester exchange catalysts. The total selectivity to MPO and DPO kept about 99.0% over TiO_2/SiO_2 and the conversion of DMO was 66.7% at 10% Ti loading, which was the maximum at different Ti loading. The structure and the chemical state of titanium species in TiO_2/SiO_2 had been investigated by XRD and XPS. The surface Ti(IV) species in the form of a monolayer was dominant until 6% Ti loading, while crystalline TiO_2 was detected at 8% Ti loading. IR of adsorbed pyridine and NH_3-TPD characterization indicated that the desirable catalytic activity of TiO_2/SiO_2 could be ascribed to its weak Lewis acid. Lewis acid sites cooperated with TiO_2 to catalyze the synthesis of MPO and DPO.

Keywords: Diphenyl carbonate; Dimethyl oxalate; Diphenyl oxalate; Methyl phenyl oxalate; Transesterification; TiO_2/SiO_2; Weak Lewis acid sites

1. Introduction

Polycarbonates (PCs) are important engineering thermoplastics with excellent mechanical and optical properties as well as electrical and heat resistance properties. They have been used in many fields as the substitutes for glass and metals. PCs have been commercially prepared by the interfacial polycondensation of bisphenol-A with phosgene. The disadvantages of the conventional phosgene process include the use of a large amount of methylenechloride as the solvent, which is about ten times the weight of the products, and a highly toxic phosgene as the reagent [1].

In recent years, there has been an increasing demand for safer and more environmentally friendly processes for PCs synthesis. One such process is composed of the synthesis of diphenyl carbonate (DPC) followed by the transesterification between DPC and bisphenol-A [2]. In this scheme, no toxic solvents are used and the by-product phenol may be recycled.

However, DPC is prepared commercially by the reaction of phenol and phosgene in the presence of bases such as sodium hydroxide [3]. Obviously, this traditional process for DPC has the same shortcomings as mentioned above because of the use of phosgene. Therefore, in order to produce PCs without social effects of pollution, the key technology is the preparation of DPC via a green process.

Several alternative methods for DPC synthesis have been developed or proposed [4–12], e.g., oxidative carbonylation of phenol and transesterification reaction. Many patents and papers covering the catalytic oxidative carbonylation of phenol have been issued over the years, but all suffer from low phenol conversions and poor diphenyl carbonate selectivity [7–12]. Dimethyl carbonate (DMC) can be also used as a substitute for phosgene in the synthesis of DPC through transesterification with phenol. Unfortunately, the transesterification reaction rate is low and the formation of azeotrope between DMC and methanol will cause separation problems [4–6].

Among non-phosgene DPC synthesis, the transesterification of dimethyl oxalate (DMO) with phenol to prepare diphenyl oxalate (DPO), followed by the decarbonylation of DPO to produce DPC, as shown in reactions (1) and (2), is

* Corresponding author. Tel.: +86-22-2740-6498; fax: +86-22-2789-0905.
E-mail address: xbma@tju.edu.cn (X. Ma).

1381-1169/$ – see front matter © 2004 Elsevier B.V. All rights reserved.
doi:10.1016/j.molcata.2003.12.020

an available route [13,14].

$$(COOCH_3)_2 + 2C_6H_5OH \rightarrow (COOC_6H_5)_2 + 2CH_3OH \quad (1)$$

$$(COOC_6H_5)_2 \rightarrow CO(OC_6H_5)_2 + CO \quad (2)$$

This method is more effective because no azeotrope is formed in the reaction system; thus, co-products of methanol and CO can be separated more easily compared with the synthesis of DPC by the transesterification of DMC with phenol. The methanol and CO produced in the transesterification and decarbonylation reaction can also be reusable in the dimethyl oxalate production via oxidative carbonylation of methanol as shown in reaction (3) [15].

$$2CO + 2CH_3OH + \tfrac{1}{2}O_2 \rightarrow (COOCH_3)_2 + H_2O \quad (3)$$

A pilot plant test in DMO production has been completed by Ube Industries and the technology for large-scale commercial production has been established. And one of the possible applications of this process is to supply DMO for the preparation of DPC [16].

For the synthesis of DPC from the transesterification of DMO with phenol, the decarbonylation of DPO to produce DPC could be carried out easily over PPh_4Cl catalyst, and the yield of DPC may be up to 99.5% [17,18]. However, the synthesis of DPO from the transesterification of phenol with DMO follows two-step reaction module consisting of the transesterification of DMO with phenol into methyl phenyl oxalate (MPO), and then the production of DPO via a further transesterification or the disproportionation of MPO, as shown in the following reaction.

$$(COOCH_3)_2 + C_6H_5OH \rightarrow C_6H_5OOCCOOCH_3 + CH_3OH \quad (4)$$

$$C_6H_5OOCCOOCH_3 + C_6H_5OH \rightarrow (COOC_6H_5)_2 + CH_3OH \quad (5)$$

$$2C_6H_5OOCCOOCH_3 \rightarrow (COOC_6H_5)_2 + (COOCH_3)_2 \quad (6)$$

The thermodynamic equilibrium constants of reactions (4)–(6) at 453 K are only 0.23, 4.77×10^{-8} and 2.09×10^{-7}, respectively, as determined from the thermodynamic calculations made with group contribution on liquid components. This indicates that the transesterification between dimethyl oxalate and phenol, especially a further transesterification of MPO with phenol and the disproportionation of MPO are not favorable in the thermodynamics. The equilibrium conversion of DMO is only 32.4% based on Eq. (4).

Generally, the transesterification of DMO with phenol is carried out in the liquid phase using homogeneous catalysts such as Lewis acids or soluble organic Pb, Sn, or Ti compounds [13,14]. Unfortunately, in these homogeneous transesterification systems, the separation of the catalysts from the products will be complicated when these catalyst systems are applied into the industrial process. Therefore, the development of active solid catalysts is highly desirable in view of regeneration and separation. However, there are few reports on the development of active heterogeneous catalysts for the reaction.

In this work, we propose the synthesis of DPC from the transesterification of DMO with phenol over TiO_2/SiO_2 catalyst. TiO_2/SiO_2 exhibited the better activity and excellent selectivity to MPO and DPO in the transesterification of DMO and phenol.

2. Experimental

2.1. Catalysts preparation

To prepare TiO_2/SiO_2 catalysts, SiO_2 samples with various Ti loadings, given in weight percentage based on metal, were impregnated with a solution of tetrabutoxytitanium dissolved in toluene for 24 h. And then these pretreated samples were dried in an oven for 2 h at 393 K and calcined in a muffle furnace at 823 K for 4 h.

2.2. Transesterification of DMO with phenol

The transesterification of DMO with phenol was carried out in a three-neck flask (250 ml) equipped with a distillation apparatus and a thermometer. Owing to the use of a distillation column and the continuous separation of co-product methanol from the reaction, the thermodynamic equilibrium limitation in reaction (1) was avoided. The reaction mixture contained 0.1 mol DMO, 0.5 mol phenol and 1.8 g TiO_2/SiO_2 catalyst. After the raw materials and catalyst were placed into the batch reactor, nitrogen gas was flowed at 30 SCCM to purge the air from the reaction system. After 10 min, nitrogen was stopped and the flask was heated at a rate of 10 K min^{-1}. The reaction was conducted at 453 K and atmospheric pressure. Qualitative and quantitative analysis of reaction products and distillates were carried out on a HP 5890-HP5971MSD and a HP 5890 gas chromatograph equipped with a flame ionization detector (FID). An OV-101packed column was used to separate products for GC analysis. The selectivity to MPO and DPO was defined as the moles of MPO and DPO produced per 100 mol of consumed DMO, and the yields of MPO and DPO were obtained from multiplication of DMO conversion by the selectivity to MPO and DPO.

2.3. Characterization of TiO_2/SiO_2 catalyst

The IR spectroscopic measurements of adsorbed pyridine were carried out on a Bruker VECTOR22 FTIR spectrometer. The scanning range was from 500 to 4000 cm^{-1} and the resolution was 4 cm^{-1}. The sample powder was pressed into a self-supporting wafer.

Powder X-ray diffraction (XRD) measurements were conducted on a MAC Science D/Max-2500 X-ray diffractometer using a radiation source of Cu Kα (λ = 1.5405 Å) at 40 kV and 100 mA with a scanning rate of 8° min^{-1}.

NH_3-TPD spectra were recorded using a Micromeritics 2910 chemical adsorption spectrometer. Samples were purged with argon at 423 K for 1 h and then cooled to ambient temperature. The pulses of ammonia were supplied to the samples to saturate. Ammonia was replaced with argon and sample was heated to 873 K at a rate of 10 K min^{-1}.

The specific surface areas and the pore size distribution of the catalysts were determined on a constant volume adsorption apparatus (CHEMBET-3000) by the N_2 BET method at liquid nitrogen temperature. The pore size distribution was calculated using the theory of BJH.

3. Results and discussion

3.1. Catalytic property of TiO_2/SiO_2 catalyst

Table 1 showed the catalytic properties of TiO_2, SiO_2 and TiO_2/SiO_2 for the transesterification of DMO with phenol. For TiO_2, the total selectivity of MPO and DPO was 99.4% with DMO conversion of 32.1% as well as MPO yield of 25.7% and DPO yield of 6.3%. For SiO_2, the selectivity of MPO was up to 100%, while the conversion of DMO was only 1.7%. Both of them performed the better selectivities than all conventional ester exchange catalysts, such as $ZnCl_2$, $AlCl_3$, $MgCl_2$, $Zn(OAc)_2$, $Ti(OC_4H_9)_4$ and $SnOBu_2$, etc. [19]. However, The conversion of DMO was not high over TiO_2 and SiO_2. We have also reported the total selectivity of MPO and DPO was 99% over TS-1 [19] and MoO_3/SiO_2 [20,21], while DMO conversion was 26.5 and 54.6%, respectively. When TiO_2 was supported on SiO_2, it was found that TiO_2/SiO_2 exhibited the favorable activity and selectivity for the transesterification of DMO with phenol. The total selectivity of MPO and DPO was kept at 99% and the conversion of DMO improved significantly over TiO_2/SiO_2, compared with the catalysts mentioned above. The conversion of DMO was improved greatly from 45.6 to 66.7% with the increase of Ti loading from 1 to 10% based on metal, while the total selectivity to MPO and DPO kept steady at about 99%. Accordingly, the yields of MPO and DPO were improved. The conversion of DMO and the yields of MPO and DPO showed the maxima at 10% Ti loading, beyond which both the conversion and the yield decreased.

Table 1
The catalytic properties of TiO_2/SiO_2 catalysts with different Ti loading

Ti loading (wt.%)	Conversion (%) DMO	Selectivity (%)			Yield (%)	
		AN	MPO	DPO	MPO	DPO
1	45.6	0.5	80.9	18.6	36.9	8.5
2	48.2	0.7	80.3	19.0	38.7	9.2
4	53.2	0.7	82.0	17.3	43.6	9.2
6	54.5	0.8	81.8	17.4	44.6	9.5
8	57.1	1.0	82.5	16.5	46.5	10.0
10	66.7	0.5	73.0	26.5	48.7	17.7
12	58.3	0.5	74.0	25.4	43.1	14.8
14	51.1	0.6	76.2	23.2	38.9	11.9
16	38.5	0.8	80.0	19.2	30.8	7.4
TiO_2	32.1	0.6	79.9	19.5	25.7	6.3
SiO_2	1.7	0	100.0	0	1.7	0

Reaction condition: 0.1 mol DMO, 0.5 mol phenol, 1.8 g catalyst, conducted at 180 °C for 2 h. MPO: methyl phenyl oxalate, DPO: diphenyl oxalate, AN: anisole.

For the disproportionation of MPO into DPO and the further transesterification of MPO into DPO, the catalytic activities of TiO_2/SiO_2 catalysts were still low. Therefore, the transesterification reaction to produce DPO was inhibited by a great deal of MPO intermediate because MPO could not make a further transformation into DPO. The experimental results also showed that the DMO conversion increased after 2 h. However, the increase of the DMO conversion was not in direct proportion to the increase of the reaction time. In order to get convenient comparison from the activities of various catalysts, we carried out the reaction for 2 h to obtain all the data involved in this paper.

Moreover, to make further improvement of DMO conversion and the selectivity to DPO, the further research about transforming of MPO into DPO is designed. MPO is removed from the reaction system by distillation column and the disproportionation of MPO into DPO is carried out over suitable disproportionation catalysts in another reactor. The research is underway.

3.2. IR characterization of adsorbed pyridine

IR analysis of adsorbed pyridine allows a clear distinction between Brõnsted and Lewis acid sites. The absorption bands, appearing at 1545 and 1455 cm^{-1} in the IR spectra, are assigned to adsorbed pyridine coordinated with Brõnsted and Lewis acid sites, respectively. The peak at 1490 cm^{-1} can be ascribed to the overlapping of Brõnsted acid and Lewis acid sites [22–24]. Fig. 1 showed the adsorbed pyridine IR spectra of the TiO_2/SiO_2 at different Ti loading. It can be seen that IR pyridine adsorption spectra of TiO_2/SiO_2 had peaks at 1455 and 1490 cm^{-1}, while the peak at 1545 cm^{-1} was absent. This indicated that there were only Lewis acid sites, but no Brõnsted acid sites on TiO_2/SiO_2. When Ti loading was increased, there only existed Lewis acid sites, indicating that the amount of Ti loading had no influence on the kind of acid sites. So it can be concluded that Lewis acid sites were the active center for the transesterification of DMO with phenol to produce MPO and DPO, which was similar to TS-1 [19].

3.3. Temperature-programmed desorption of NH_3

Temperature-programmed desorption of NH_3 (NH_3-TPD) characterization was conducted to survey the acid strength of TiO_2/SiO_2. In the NH_3-TPD curves, peaks are generally

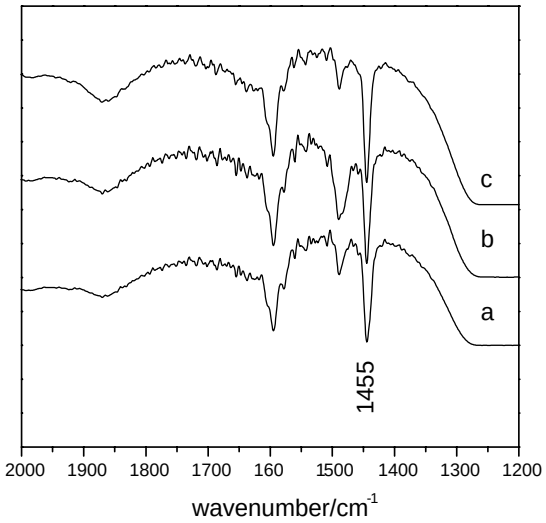

Fig. 1. IR spectra of pyridine absorbed on TiO_2/SiO_2 catalysts with different Ti loading: (a) 8% TiO_2/SiO_2; (b) 10% TiO_2/SiO_2; (c) 12% TiO_2/SiO_2.

distributed into two regions, below and above 673 K referred to low-temperature (LT) and high-temperature (HT) region, respectively [25,26]. The peaks in the HT and LT region can be attributed to the desorption of NH_3 from strong and weak acid sites, respectively. From the results shown in Fig. 2, it could be found that the peaks only appeared in the low-temperature region of each absorbed curve. This indicated that there only existed weak acid sites on TiO_2/SiO_2 and the loading amount of Ti gave no apparent impact on strength of the acid sites. Because the weak acid sites were in favor of the formation of MPO and DPO [21], the high selectivity of MPO and DPO was obtained over TiO_2/SiO_2. As shown in Table 2, the amount of acid sites increased with the increasing of Ti loading from 1 to 8%, indicating that

Table 2
Amount of NH_3 desorbed at low temperature on TiO_2/SiO_2 catalysts

Ti loading (wt.%)	Amount of desorbed NH_3 (mmol NH_3/g catalyst)
1	0.361
2	0.424
4	0.721
6	0.761
8	0.863
10	0.731
12	0.748
14	0.734
16	0.744

the new acid sites were formed due to the adding of TiO_2 at lower loading.

3.4. Analysis of X-ray diffraction

The structure and the chemical state of Ti species in TiO_2/SiO_2 had been investigated by means of X-ray diffraction as shown in Fig. 3. It was observed that the titanium phase was not observed by XRD below 8% Ti loading, yet weak XRD peaks of anatase were detected at higher loadings. Therefore, it was possible for the surface Ti(IV) species to form the small particles or highly disperse below 8% Ti loading. The curve (j) in Fig. 3 was the results of nano-TiO_2 mixing with SiO_2 with 1 wt.% Ti content. The particle size of nano-TiO_2 was only 15–30 nm. The characterization results for it showed that the clear peaks of anatase were detected by XRD. According to this result, for TiO_2/SiO_2, the particle size of TiO_2 below 8% Ti loading was smaller than 15 nm because no XRD peaks of anatase were detected. Furthermore, TiO_2 should be highly dispersed at the silica surface. Therefore, we think the reason for the lack of XRD

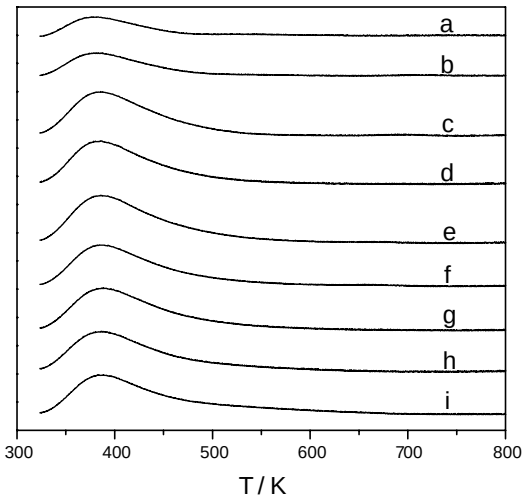

Fig. 2. NH_3-TPD profile of TiO_2/SiO_2 catalysts with different Ti loading: (a) 1%; (b) 2%; (c) 4%; (d) 6%; (e) 8%; (f) 10%; (g) 12%; (h) 14%; (i) 16%.

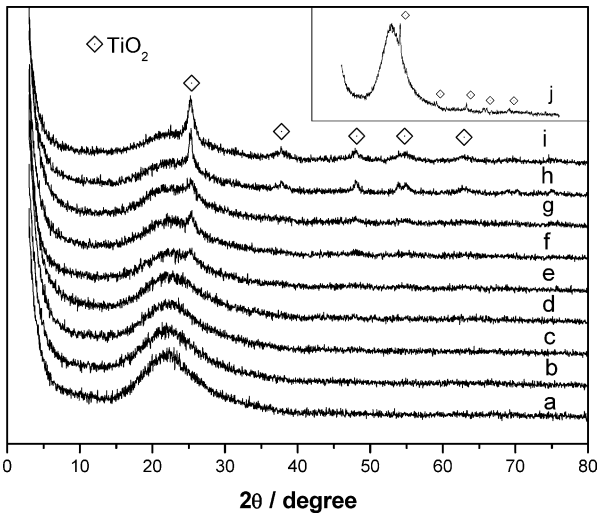

Fig. 3. XRD spectra of TiO_2/SiO_2 catalyst with different Ti loading: (a) 1%; (b) 2%; (c) 4%; (d) 6%; (e) 8%; (f) 10%; (g) 12%; (h) 14%; (i) 16%; (j) 1% nano-TiO_2/SiO_2.

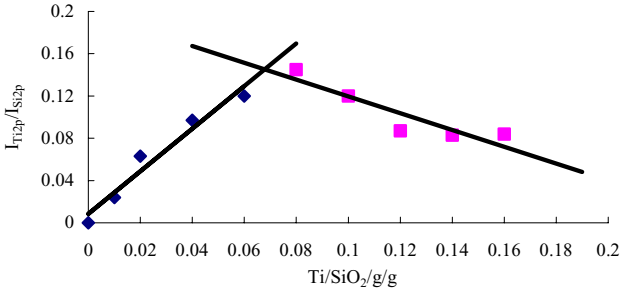

Fig. 4. Correlation between $I_{Ti(2p)}/I_{Si(2p)}$ with different Ti loading of TiO_2/SiO_2 catalysts.

peak of titania at low Ti loading is not the broad XRD peaks attributed by the small particles, but the high dispersion of TiO_2 at the surface.

3.5. Analysis of X-ray photoelectron spectroscopy

The investigation of binding energy and intensity of some surface elements by X-ray photoelectron spectroscopy (XPS) give the information of the chemical states and relative quantities of the outermost surface compounds. The Ti $2p_{3/2}$ binding energies of the TiO_2/SiO_2 catalysts were invariant with Ti loading in the range of 458.3 ± 0.2 eV, which was corresponded to the binding energy of titanium dioxide.

Based on the theory proposed by Kerkhof and Moulijn [27], a linear relation between the relative XPS intensity and the bulk ratio of the metal and the support may be expected for monolayer catalysts as well as for catalysts with crystallites of constant sizes. Point of intersection of two lines showed the change from the monolayer to the crystallite. The theory was widely used in the research of metal oxide supported catalysts [28–30]. As shown in Fig. 4, two linear lines intersected at 7.1% Ti loading. Therefore, surface Ti(IV) species was in the form of a monolayer at 6% Ti loading, but crystalline TiO_2 was formed at 8% Ti loading. This was accordant with the results of XRD.

Connected with the results of NH_3-TPD, the amount of acid sites were invariant at higher Ti loading because further added TiO_2 mainly contributed to the growth of crystal phase. However, the DMO conversion still increased when crystalline TiO_2 was appeared because crystalline TiO_2 was also an active and selective catalyst for the transesterification. Lewis acid sites cooperated with crystalline TiO_2 to catalyze the transesterification of DMO with phenol at higher Ti loading. But, the conversion of DMO was decreased when a great deal of crystalline TiO_2 formed.

3.6. Pore size distribution and specific surface area

Using the 3D model of Material Studio 2.2 edition molecular simulation software packages, the molecular sizes of DMO, phenol, MPO, and DPO were obtained. The molecular sizes of DMO and phenol were $X = 6.4$ Å, $Y = 5.1$ Å and $X = 7.1$ Å, $Y = 4.9$ Å, $Z = 2.5$ Å, respectively. And

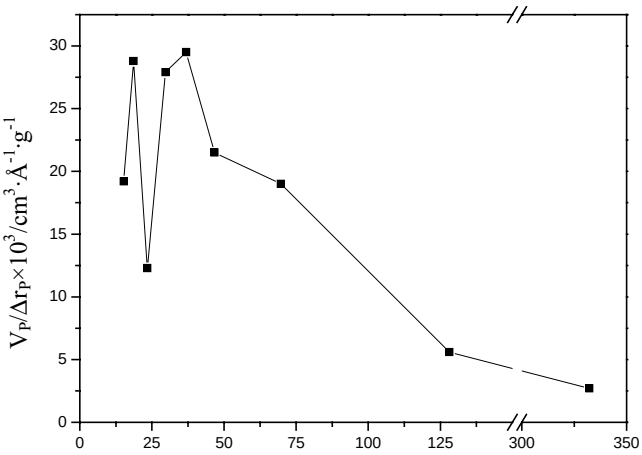

Fig. 5. Pore size distribution of 10% TiO_2/SiO_2.

the molecular size of the formed MPO and DPO were $X = 8.4$ Å, $Y = 6.3$ Å, $Z = 5.6$ Å and $X = 9.9$ Å, $Y = 5.7$ Å, $Z = 4.6$ Å, respectively. Fig. 5 illustrates the pore size contribution of 10% TiO_2/SiO_2. The pore size distribution testing presented that the pore size range of TiO_2/SiO_2 was main 25–130 Å. Therefore, the molecular of DMO and phenol could access the pores of TiO_2/SiO_2 freely. At the same time, the produced MPO and DPO could return the reaction liquid, making the active sites used effectively. So, the transesterification of DMO with phenol occurred on the inter and outer surface of catalyst simultaneously, which accelerated the improvement of DMO conversion.

The data of specific surface area of catalysts are presented in Table 3. When TiO_2 was supported on SiO_2, the specific surface area increased largely compared with that of TiO_2. Although the specific surface area of TiO_2 was very small, the specific surface area of TiO_2/SiO_2 were about 230 $m^2\ g^{-1}$, close to the specific surface area of SiO_2. TiO_2/SiO_2 showed higher activity for the transesterification of DMO with phenol compared with TiO_2. TiO_2 active centers to be dispersed on the surface of the carriers were in favor of transesterification reaction. Because a great deal of crystalline TiO_2 was formed at higher Ti loading, the specific surface area of TiO_2/SiO_2 decreased, resulting in the decrease of the catalytic activity.

Table 3
Surface area of the catalyst samples

Ti loading (wt.%)	A (m^2/g)
TiO_2	11.1
SiO_2	231.1
1	208.7
2	228.2
4	230.1
6	243.5
8	252.4
10	254.4
12	239.7
14	186.7
16	178.9

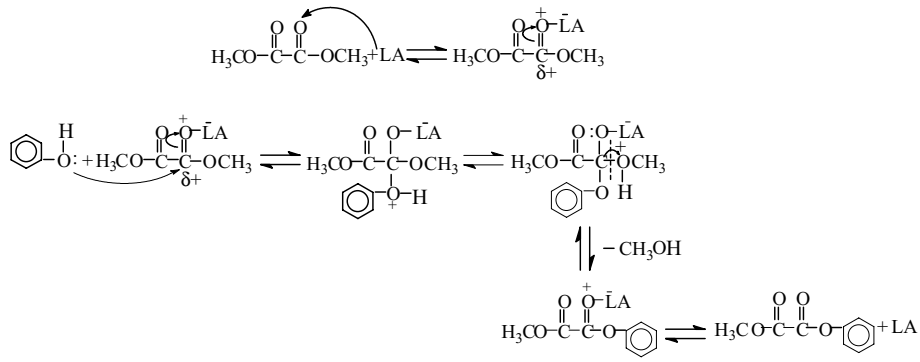

Scheme 1.

3.7. Reaction mechanism

As shown in Scheme 1, the acid mechanism of the transesterification of dimethyl oxalate with phenol to MPO over TiO_2/SiO_2 was proposed. The weak Lewis acid sites favored the formation of MPO. The reaction course was according to the cleavage of acyloxy bonds. The carbonyl in DMO molecule was not easily attacked by weak nucleophilic reagent, phenol, because of its low activity. However, carbonium ion could be formed in the presence of the weak Lewis acid sites. Therefore, carbon atom in carbonyl possessed higher positive charge, which was propitious for attacking of phenol. Finally, ester exchange was completed along with the formation of methanol.

Considering stereochemistry, oxo-reaction occurred on Π electron plane. And the nucleophilic reagent vertically attacked Π plane. And from steric effect, the carbonylic activity was decreased in nucleophilic addition reaction owing to the great volume of the groups linked with carbonyl. For DMO, the group connected with carbonyl was –COO–. So, the activity of MPO synthesis from the transesterification of DMO with phenol was not very high. Especially, after the formation of MPO, the volume of the groups jointed with carbonyl was further increased, leading to the difficulty of MPO translating to DPO. This was consistent with the experimental data, in which the yield of DPO was less than the yield of MPO.

4. Conclusions

TiO_2/SiO_2 was an active catalyst for the synthesis of methyl phenyl oxalate and diphenyl oxalate from the transesterification of dimethyl oxalate with phenol. The conversion of DMO was 66.7% and the selectivity to MPO and DPO was 73.0 and 26.5% at 10% Ti loading, which were the maxima at the different Ti loading. IR of adsorbed pyridine and NH_3-TPD characterization indicated that the desirable catalytic activity of TiO_2/SiO_2 could be ascribed to its weak Lewis acid. The structure and the chemical state of titanium species in TiO_2/SiO_2 had been investigated by XRD and XPS. The surface Ti(IV) species in the form of a monolayer was dominant until 6% Ti loading, while crystalline TiO_2 was detected at 8% Ti loading. Lewis acid sites cooperated with TiO_2 to catalyze the synthesis of MPO and DPO.

Acknowledgements

Supports from National Natural Science Foundation of China (No. 20276050), Tianjin Science and Technology Committee (TSTC) of China (No. 033103511), and Foundation for University Key Teacher by the Ministry of Education are very much appreciated.

References

[1] D. Freitag, U. Grico, P.R. Muller, in: H.F. Mark (Ed.), Polycarbonate in Encyclopedia of Polymer Science and Engineering, vol. 11, Wiley, New York, 1987, p. 649.
[2] Y. Ono, Pure Appl. Chem. 68 (1996) 367.
[3] M. Janatpour, S.J. Shafer, EP 228672 (1987).
[4] W.B. Kim, J.S. Lee, J. Catal. 185 (1999) 307.
[5] Z.H. Fu, Y. Ono, J. Mol. Catal. A 118 (1997) 293.
[6] W.B. Kim, J.S. Lee, Catal. Lett. 59 (1999) 83.
[7] I. Gabriello, R. Ugo, T. Renato, Ger. Offen. 2528412 (1976).
[8] W. Akinobu, O. Yoshiyuki, T. Hideaki, JP 11 279126 (1999).
[9] M.H. Oyevaar, B.W. To, M.F. Doherty. US Patent 6093842 (2000).
[10] T. Hideaki, O. Yoshiyuki, M. Atusi, EP 684221 (1995).
[11] A.J. Chalk, Ger. Offen. 2738520 (1978).
[12] K. Kongen, C. Arihito, S. Kashun, JP 08 198815 (1996).
[13] N. Keigo, T. Shuji, H. Katsumasa, S. Ryoji, US Patent 5834651 (1998).
[14] N. Keigo, T. Shuji, H. Katsumasa, S. Ryoji, S. Akinori, W. Katsutoshi, US Patent 5922827 (1999).
[15] T. Matsuzaki, A. Nakamura, Catal. Surv. Jpn. 1 (1997) 77.
[16] S. Vchtumi, K. Ataka, T. Matsuzaki, J. Organomet. Chem. 576 (1999) 279.
[17] H. Katsumasa, S. Ryoji, K. Kashiwagi, US Patent 5892089 (1998).
[18] S.P. Wang, X.B. Ma, Z.H. Li, G.H. Xu, Nat. Gas Chem. Eng. (China) 27 (2002) 1.
[19] X.B. Ma, H.L. Guo, S.P. Wang, Y.L. Sun, Fuel Process Technol. 83 (2003) 275.
[20] J.L. Gong, X.B. Ma, S.P. Wang, M.Y. Liu, X. Yang, G.H. Xu, J. Mol. Catal. A: Chem. 207 (2004) 215.

[21] X.B. Ma, J.L. Gong, S.P. Wang, Catal. Commun. 5 (2004) 101.
[22] G.N. Vayssilov, Catal. Rev. 39 (1997) 209.
[23] T. Barzetti, E. Selli, D. Moscotti, L. Forni, J. Chem. Soc., Faraday Trans. 92 (1996) 1401.
[24] T.R. Hughes, H.M. White, J. Phys. Chem. 71 (1967) 2192.
[25] C.A. Emeis, J. Catal. 141 (1993) 347.
[26] M. Sawa, M. Niwa, Y. Murakami, Zeolites 10 (1990) 532.
[27] F.B. Kerkhof, J.A. Moulijn, J. Phys. Chem. 83 (1979) 1612.
[28] N. Escalona, J. Ojeda, Appl. Catal. A: Gen. 234 (2002) 45.
[29] Y.C. Xie, Y.Q. Tang, Adv. Catal. 37 (1990) 1.
[30] L. Salvati Jr., L.E. Makovsky, J.M. Stencei, F.R. Brown, D.M. Hercules, J. Phys. Chem. 85 (1981) 3700.